nature communications

Article

https://doi.org/10.1038/s41467-024-52893-3

Tuneable mesoporous silica material for hydrogen storage application via nano-confined clathrate hydrate construction

Received: 9 February 2024

Accepted: 16 September 2024

Published online: 08 October 2024

Check for updates

Radu-George Ciocarlan[1], Judit Farrando-Perez[2], Daniel Arenas-Esteban[3], Maarten Houlleberghs[4], Luke L. Daemen[5], Yongqiang Cheng[5], Anibal J. Ramirez-Cuesta[5], Eric Breynaert[4], Johan Martens[4], Sara Bals[3], Joaquin Silvestre-Albero[2] & Pegie Cool[1]

Safe storage and utilisation of hydrogen is an ongoing area of research, showing potential to enable hydrogen becoming an effective fuel, substituting current carbon-based sources. Hydrogen storage is associated with a high energy cost due to its low density and boiling point, which drives a high price. Clathrates (gas hydrates) are water-based (ice-like) structures incorporating small non-polar compounds such as H_2 in cages formed by hydrogen bonded water molecules. Since only water is required to construct the cages, clathrates have been identified as a potential solution for safe storage of hydrogen. In bulk, pure hydrogen clathrate (H_2O-H_2) only forms in harsh conditions, but confined in nanospaces the properties of water are altered and hydrogen storage at mild pressure and temperature could become possible. Here, specifically a hydrophobic mesoporous silica is proposed as a host material, providing a suitable nano-confinement for ice-like clathrate hydrate. The hybrid silica material shows an important decrease of the pressure required for clathrate formation (approx. 20%) compared to the pure H_2O-H_2 system. In-situ inelastic neutron scattering (INS) and neutron diffraction (ND) provided unique insights into the interaction of hydrogen with the complex surface of the hybrid material and demonstrated the stability of nano-confined hydrogen clathrate hydrate.

The worldwide increase in energy consumption drives the science and engineering communities to engage in a quest for the "ideal" energy source. Energy can be stored in four specific forms, i.e. nuclear fuel, mechanical energy, in systems that incorporate electric or magnetic fields, and chemical energy[1]. At present, the most common form of energy used in day-to-day situations is chemical energy, derived from fossil fuels, batteries, or alternative sources such as biogas, hydrogen, or ammonia[2]. The transition to biofuels and electricity is an important step to reduce the world's dependence on fossil fuels, but ultimately will be insufficient to satisfy societies energy and transportation requirements.

A possible solution is to use the hydrogen (H_2) as energy carrier. Hydrogen not only has a gravimetric energy density far exceeding that of any carbon-based fuel (e.g., 300% with respect to gasoline or diesel),

[1]Department of Chemistry, University of Antwerp, Universiteitsplein 1, Wilrijk, Belgium. [2]The Advanced Materials Laboratory (LMA) - Department of Inorganic Chemistry – IUMA, University of Alicante (UA), Alicante, Spain. [3]Electron Microscopy for Materials Science (EMAT), NANOlab Center of Excellence, University of Antwerp, Antwerp, Belgium. [4]Centre for Surface Chemistry and Catalysis, NMRCoRe - NMR - XRAY - EM Platform for Convergence Research, Department of Microbial and Molecular Systems (M2S), KU Leuven, Celestijnenlaan 200F, Leuven, Belgium. [5]Spallation Neutron Source, Oak Ridge National Laboratory, Oak Ridge, TN, USA. e-mail: pegie.cool@uantwerpen.be

its combustion with O_2 exclusively produces pure water[3]. On a less positive note, multiple impediments prevent hydrogen from reaching its full potential as an alternative energy source. The most significant challenges are related to this future fuel's safe storage, delivery, and use. Many approaches have been explored over the years, including compressed/liquified/cryo-compressed, physically adsorbed and chemically bonded hydrogen storage (metal hydrides, complex hydrides and liquid organic hydrides). The first three methods are energetically costly, and raise safety-related concerns. Likely, none of them will ever qualify as economically efficient or achieve the societal acceptance required for their widespread implementation. Chemically bonded hydrogen storage - involving formation of a variety of chemical bonds – comes with limitations in terms of regeneration, stability, side product formation and high cost of some of the precursors[4–7].

A series of studies sparked the idea that physical adsorption of hydrogen could overcome most of the drawbacks[5,8,9]. Since weak van der Waals forces are involved in the storage process, hydrogen is reversibly interacting with the material's surface. Physisorption usually entails high rates of adsorption/desorption, whereas the enthalpy of the system and the refuelling time are not an issue. The classes of materials already studied all focus on exploiting the high surface area of microporous materials (carbon-based materials[10,11], zeolites[12,13] and metal-organic frameworks (MOFs)[14–17]). Even in these materials, the physical adsorption of hydrogen however still requires low temperatures (77 K) and/or high pressures (up to 10 MPa), and in some cases the reactants for generating the support material are not economically viable for large-scale production (MOFs).

With nature as inspiration, the scientific community explored another method for hydrogen storage, which involved trapping hydrogen molecules inside a water-based cage-like structure. In nature, large deposits of extraordinary ice-like structures trapping huge amounts of methane (CH_4) or carbon dioxide (CO_2) are found. This molecular enclathration occurs at moderate temperature and pressure for larger molecules, whereas for hydrogen, it still requires up to 200 MPa to obtain the pure H_2O-H_2 ice-like structure, known as clathrate hydrogen hydrate[18–20]. To alleviate these draconic conditions, promoters were tested and evaluated, with the most significant improvement measured for binary tetrahydrofuran (THF) – hydrogen clathrate hydrates[18,20,21]. Using promotors, however, impacts the storage capacity as the cages occupied by the promotor molecules are blocked for hydrogen storage. Some promotors also act as structure-directing agents towards formation of clathrate hydrate structures with lower hydrogen storage capacities. On top, also the toxicity of promoters and their environmental impact are also important factors to be considered for large-scale applications[22].

Recently, innovative studies reported generation of clathrate hydrates under milder conditions, when water is present in a nano-confinement environment and not as bulk[20,21,23–25]. By fractioning water in smaller volumes inside nanopores, the interfacial area between the hydrogen gas and water is greatly extended, thus having a positive impact on the clathrate hydrate formation. In the same line of thought, inside the nano-pores, the water molecules' properties are altered compared to the macroscopic level due to their interaction with the surface of the pores. Note that while this happens to a greater extent for the hydrophobic surfaces of the nano-pores, it is important to mention that these properties are also closely related to the volume and shape of the confined space[26,27]. We reported on the importance of pore surface hydrophobicity on the kinetics of methane and hydrogen clathrate formation in ordered silica materials (SBA-15, MCF)[18–20]. Casco et al. did a series of studies in which the importance of the material's hydrophobicity was discussed for the methane clathrates formation[28–31]. Moreover, a pressure reduction (approx. 30%) was observed for the pure hydrogen hydrate formation when water was encapsulated inside hydrophobic carbon pores[23].

To the best of our knowledge, this is the first report of the formation of pure hydrogen clathrate inside the pores of a hybrid, modified silica (SiO_2) at pressures reduced with ~20% as compared to what is required to form pure hydrogen clathrate hydrate in bulk, at the same temperature. A model system with a well-defined pore arrangement – mesostructured cellular foam (MCF), was surface-modified to induce hydrophobicity. The well-known hydrophilicity of the silica surface was reduced by grafting phenethyl groups on the surface. The hydrophobicity level is influenced by the type, density and size of the group grafted on the surface of silica materials[32,33]. Based on prior experiments, modifications with aliphatic chains shorter than 4-5 carbon atoms have a relatively low impact on hydrophobicity if the grafting density is not high enough (>1 group/nm^2). At the same time, aliphatic chains longer than 8 carbons may induce diffusion problems and higher pore volume reduction. Moreover, if the pores are too hydrophobic this can prevent water from entering the pores, thus inhibiting hydrates formation. The selected group (phenethyl) provides a higher surface coverage effect due to its benzene ring, with a rough distance of 6.8 Å from the Si atom to the furthest C atom, slightly lower than 6 aliphatic carbon atoms (7.8 Å) in length, and for these reasons, we believe it represents a good compromise.

Below, we present in detail a picture of the hydrogen interaction with the complex surface of the hybrid material when a clathrate hydrate is present. The possible double role of the benzene ring belonging to the phenethyl group is explored, while the stability of the hydrogen clathrate hydrate under different conditions is investigated. This study could pave the way for the design and synthesis of new hybrid materials able to store sufficient hydrogen (simultaneously in multiple sites) under affordable conditions and for different applications.

Results

Several characterisation techniques were used to confirm that the surface modification involving the hydrophobization of the MCF silica material with phenethyl trimethoxysilane was successful. The sharp peak observed in the in-situ FTIR spectrum (Fig. 1a) at 3747 cm^{-1} for the unmodified MCF is related to the presence of isolated silanol groups (stretching vibration of isolated Si-OH) on the surface of the silica[34]. By contrast, in MCFPhene this sharp peak is greatly diminished, whereas a more prominent band appears at 3618 cm^{-1}. The sharp bands just above 3000 cm^{-1} (3000–3125 cm^{-1}), 1600 cm^{-1}, 1500 cm^{-1} and 700 cm^{-1} are related to the presence of the benzene ring, while the bands just below 3000 cm^{-1} (2900 cm^{-1} and 2800 cm^{-1}) and 1454 cm^{-1} are linked to the presence of C-H stretching vibrations of the phenethyl group. Finally, the silica framework of the MCF is visible through the bands at 1084 cm^{-1}, 806 cm^{-1} and the shoulder at around 1200 cm^{-1}[35].

According to IUPAC reference reports, the nitrogen sorption analysis interpretation indicates a type IVa isotherm with a marked H1 hysteresis loop (Fig. 1b). This classification fits the description of the MCF material, with an open structure and uniform large mesopores[36]. By comparing the MCF before and after the modification, it is clear that after the surface modification, the specific surface area and the pore volume of the material decreased (560 m^2/g vs. 420 m^2/g and 1.82 cm^3/g vs. 1.55 cm^3/g). By analysing individually the adsorption and desorption branches, one can approximate the size of the pore (adsorption, ~20 nm) and the accessible window (desorption, approx. 10 nm)[37]. At the same time, the pore size distribution values for the pores and windows of the material after the modification are slightly shifted towards smaller values (Fig. 1b). Moreover, the water adsorption and desorption isotherms fall in the type V IUPAC classification (Fig. 1c), while the presence of the organic groups on the surface drastically affects the hydrophilic-hydrophobic properties, depicted in the graph by the consistent decrease in water uptake for MCFPhene.

Furthermore, the thermogravimetric (TGA, see Supplementary Fig. 2) analysis of the material after the modification shows two clear

https://doi.org/10.1038/s41467-024-52893-3

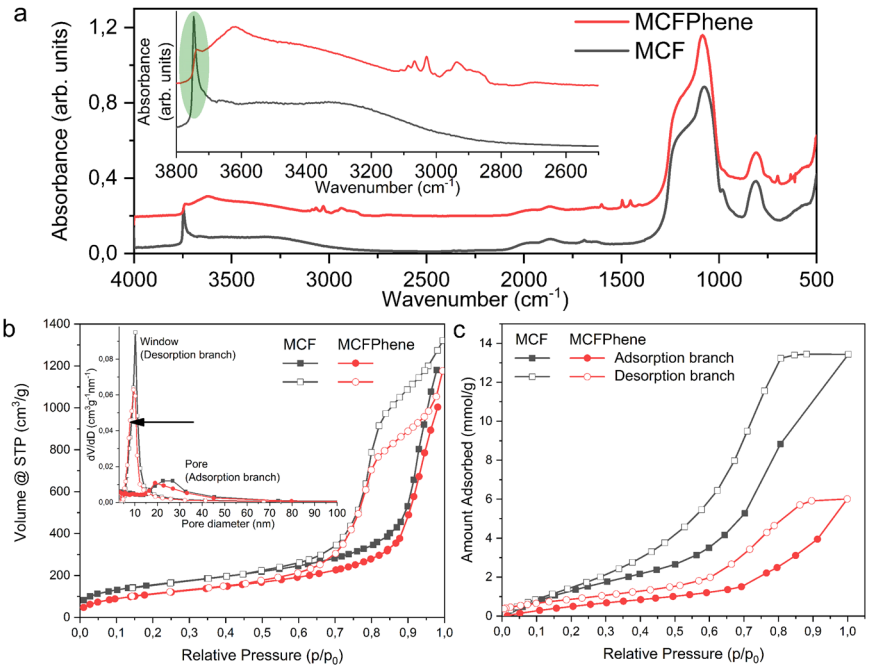

Fig. 1 | Characterisation of the silica material before and after surface modification. a FTIR spectra with the inset showing the main region specific to the surface modifications (the green area is related to the isolated silanol groups at ~3747 cm^{-1}), (**b**) N_2-sorption analyses at 77 K with the inset graph related to the pore size distribution showing the reduction of the pores after the modification (black arrow) and (**c**) water vapour sorption isotherms at 298 K before and after the MCF surface modification procedure. For (**b**) and (**c**) graphs, the hollow data points refer to the desorption branch of the isotherms, while the filled data points refer to the adsorption branch of the isotherms. Source data are provided as a Source Data File.

mass loss regions. From 363 to 493 K, the solvent and the washing agent (toluene) is expected to be mainly removed, while at higher temperatures (613–923 K), the organic groups belonging to the organosilane modifier are burned. The mass loss above 493 K is estimated to be 8%, which results in a surface coverage of approx. 0.8 groups of phenethyl molecules per nm^2.

The MCFPhene sample was further investigated by high-angle annular dark-field scanning transmission electron microscopy (HAADF-STEM) (Fig. 2a, b) and electron tomography (Fig. 2c, d) revealing a very open porous structure, with big spherical interconnected mesopores, characteristic of MCF material. A careful segmentation of the electron tomography dataset was carried out based on intensity levels and reveals that the porous structure represents 39.4% of the nanoparticle. This analysis also showed a wide variety of pore sizes with an average pore size of 19 ± 7 nm in good agreement with the N_2-sorption analysis (Fig. 2d). EDS analysis was additionally performed, showing a slightly presence of C in the sample, which supports the idea of a successful functionalisation (see Supplementary Fig. 3).

Figure 3 compares the inelastic neutron scattering spectra in the low energy transfer region for the D_2O-loaded MCFPhene sample upon pressurisation with hydrogen at 135 and 165 MPa. The spectra of a D_2O-loaded activated carbon (sample PPAC) pressurised with hydrogen at 200 MPa have been added as a reference[23]. The 135 and 165 MPa MCFPhene spectra exhibit a well-defined peak at approx. 12.3 meV. This contribution is attributed to the $J = 0$ to $J = 1$ transition of the H_2 molecular rotor interacting with the silica surface, and it is in good agreement with the work of Balderas-Xicohténcatl et al. taking into account the energy transfer values reported here and the ones reported in the work of Balderas-Xicohténcatl et al., one can conclude that the H_2 molecules are interacting with the silica surface through surface-dihydrogen interactions due to the relatively low polarizability character of the H_2 molecules[38]. In addition, the sample pressurised at 135 MPa exhibits a broad low-energy contribution (5–10 meV), most likely associated with isolated hydrogen molecules in large voids or cavities, which are the most probable heterogeneous structural defects in the ice network. An increase in the hydrogen pressure to 165 MPa gives rise to two distinct features, a doublet at 8–10 meV and a significant contribution at 14.6 meV. The comparison with the well-established PPAC-activated carbon clearly reflects that these contributions are clear fingerprints of hydrogen enclathration in hydrates. More specifically, the doublet corresponds to the rattling mode of orthohydrogen trapped inside the hydrate cages (big and small cages, respectively). At the same time, the 14.6 meV contribution is due to the rotational transition of parahydrogen to orthohydrogen (J 0 -> 1) in the clathrates. These peaks constitute a clear proof of the potential of MCF silicas to act as nanoreactors to promote the nucleation and growth of hydrogen clathrates at ≥165 MPa. The spectrum of the MCFPhene sample at 165 MPa also shows two contributions at low energy transfers (1.75 and 4.75 meV), which could be hydrogen molecules (orthohydrogen) trapped in defective cavities, most probably associated with clathrates (these peaks only appear after the clathrate formation). This observation agrees with the limited D_2O-to-hydrate yield as compared to the PPAC-activated carbon and the presence of defective crystals in the confined environment. Indeed, the nucleation mechanism is more complex for the silica sample due to the coexistence of non-reacted D_2O/ice (D_2O), hydrogen clathrates and hydrogen molecules directly interacting with the silica surface (most probably a layer of hydrogen molecules between the silica surface and the water network) inside the cavities.

As INS and neutron diffraction data are acquired simultaneously at the VISION beamline, one can confirm (Fig. 4, left) the formation of the sII clathrate when the experimental pressure reaches 165 MPa. The reflections characteristic of the sII clathrate structure are found at 2.88, 3.01, 3.28, 3.47, 4.92 and 5.14 Å, while the features belonging to hexagonal ice (Ice Ih) are seen at 3.44, 3.65 and 3.89 Å. On the contrary, when the experiment was carried out at 135 MPa, it was clear that the clathrate structure was not formed. Moreover, it appears that when comparing the 135 MPa and 0 MPa experiments, the hexagonal ice structure displays a considerably smaller peak intensity at 3.44 Å.

https://doi.org/10.1038/s41467-024-52893-3

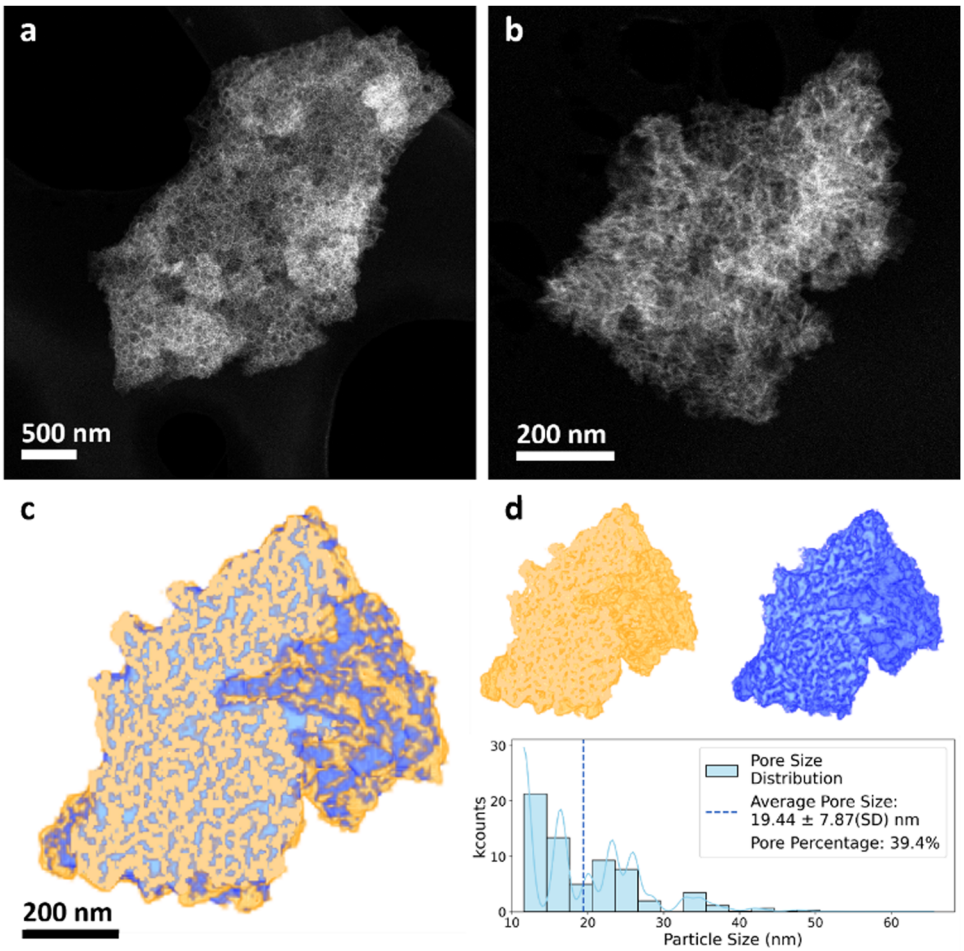

Fig. 2 | Textural and morphological details of the modified MCF material. **a**, **b** High-angle annular dark field-scanning transmission electron microscopy (HAADF-STEM) images of two MCFPhene porous particles. **c** Section of the 3D reconstruction volume for the particle in Figure (**b**), (**d**) Separate segmentation for the material and pore volumes in yellow and blue colours respectively, together with the segmentation statistics.

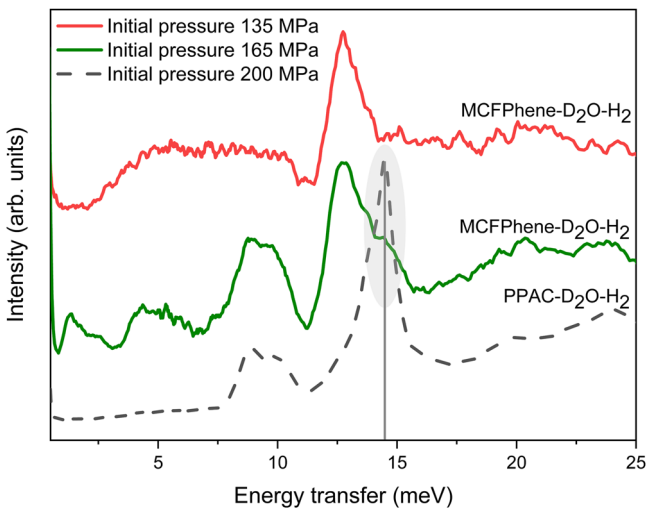

Fig. 3 | Comparison of the INS spectra at different pressures and two materials i.e. MCFPhene (silica) and PPAC (carbon). Inelastic scattering spectra of the MCFPhene-D_2O-H_2 system after different pressure experiments and measured at 0.1 MPa and 5 K (top). The INS spectra of a high-surface area activated carbon material (PPAC-D_2O-H_2, bottom, intensity divided by 20x) is included for comparison[23]. The grey line and area highlight the region (14.6 meV) that confirms the clathrates hydrates formation. Source data are available as a Source Data File.

These defective ice structures formed under high-pressure conditions could explain the presence of large voids or cavities able to accommodate hydrogen molecules (non-forming clathrates), with the associated rattling modes at low energy transfer. Supplementary Fig. 4 compares the ND pattern for the MCFPhene sample with the PPAC-activated carbon. This comparison confirms the perfect match in the position of the different crystallographic peaks for hexagonal ice and sII clathrates, independently of the evaluated host structure. However, this comparison reflects that upon pressurisation (135 MPa and above), the intensity of the peaks associated with hexagonal ice are altered for silica (the contribution at 3.44 Å vanishes), thus confirming the defective nature of the ice and clathrate nanostructures confined in silica. Finally, ND also confirms the lower water-to-hydrate yield in the case of silica compared to the activated carbon sample (nearly 100% conversion).

To check the stability of the clathrate at a higher temperature for the 165 MPa experiment, two distinct experiments were performed at 5 K, followed by an increase in temperature to 280 K, both at 0.1 MPa. Interestingly, with the rise in temperature up to 280 K, no significant differences were observed in the diffractograms (Fig. 4, right). A comparable temperature-related series of experiments were performed at 0.1 MPa after the pressure was increased up to 135 MPa (Supplementary Fig. 5). Upon comparing the neutron diffraction results, no significant changes were observed between the experiments performed after the sample reached 5 K and 280 K.

https://doi.org/10.1038/s41467-024-52893-3

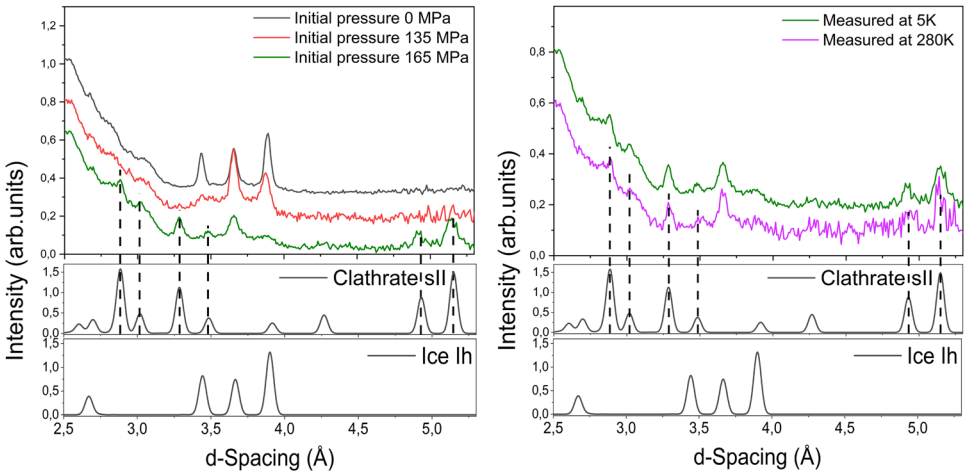

Fig. 4 | ND data at different initial pressures and temperatures. Neutron diffraction of the MCFPhene-D_2O-H_2 system after in-situ synthesis at different pressures and measured at 0.1 MPa and 5 K (left). Stability experiments for 165 MPa experiment, measured at 0.1 MPa (right). Source data are provided as a Source Data File.

Discussion

The selection of a mesoporous silica material is based on the ability to tune this type of material in terms of pores size, uniformity of the pores network, and the simplicity of altering the surface properties. More precisely, the MCF material offers a series of advantages for studying and possible extension to large-scale storage applications of H_2 as clathrates due to its high pore volume, large uniform spherical mesopores of around 20 nm, and windows of approx. 10 nm, with an open structure, results in an easily accessible SiO_2 network. The high pore volume is crucial for the water uptake of the material and the amount of H_2 clathrate that can be formed. The large pores and the accessible arrangement, demonstrated by electron microscopy, enable the growth and extent of the clathrate crystals network. In contrast, the relatively narrow distribution of the pores provides an ideal system to model the formation of the hydrates inside confined spaces.

The surface modification is applied with the main attribute of inducing hydrophobicity on the superficial layer of the silica material. To avoid much of the polymerisation of the silane and to create a homogeneous coverage with the organic molecule, before the modification, the MCF is dried (473 K), and the experimental procedure takes place under an inert atmosphere (Ar). Upon analysing the in-situ FTIR spectra, one can deduce that the reduced band at 3747 cm^{-1} for the MCFPhene sample suggests the chemical bonding of the silane to the surface of the silica. In contrast, the newly formed band and the slight difference in the region between 3600-3200 cm^{-1} are related to modifying the Si-OH surroundings. The presence of distinct spectral signatures associated with the silane compound used for surface modification, even after elevated temperature (393 K) and vacuum are applied, clearly demonstrates the existence of the intended surface modification. This idea is also supported by the N_2-sorption and TGA results, which show a slight decrease in the pore size distribution after the modification. At the same time, the mass loss centred at 673 K is considered relatively high to not belong to chemically-bonded organic groups (approx. 8% C content). The observations above and the C content detected by EDS agree with the fact that a relatively small amount of groups are attached to the surface, of the order of 0.8 groups/nm^2.

Moreover, the small difference observed in the BJH pore size distribution graph is caused by the number of groups on the surface and their properties. The phenethyl group size from the attached Si atom in the SiO_2 network to the furthest benzene ring C is about 6.8 Å. In contrast, the ethyl group provides a high degree of mobility, allowing the benzene ring to bend towards the surface of the silica.

From the INS spectra, it is clear that hydrogen molecules interact with different sites when loaded at higher pressures and in the presence of the MCFPhene material and heavy water (D_2O). The diminished reflection at 3.44 Å, under pressure conditions (135 and 165 MPa), visible in neutron diffraction results (Fig. 4), describes a possible loss of the ice structure, a transition towards the cubic ice structure, or the effect of the confinement on the ice. The entire process may be regarded, in simple terms, as a transition phase between the regular hexagonal ice structure and the sII clathrate structure formed in the presence of H_2. The simultaneous presence of both diffraction patterns (hexagonal ice and sII clathrate) at 165 MPa proves that not all the heavy water is converted into a clathrate structure. A possible explanation is that the heavy water from different sites interacts very specifically with the local environment. Thus, some sites may promote the formation of the clathrates at lower pressures than others. It is not easy to assess which site inhibits the clathrate formation. However, one can assume that due to the relatively low surface coverage, part of the heavy water forms a stronger interaction with the silica surface via hydrogen bonds, limiting the interface between the hydrogen and heavy water. On the contrary, the hydrophobic sites of the benzene rings may have the opposite effect on this by promoting hydrogen-heavy water interactions. On top of this, the possibility of extra H_2 stored as physisorbed on the silica wall surface should not be underestimated. The hydrogen adsorption capacity of the two silicas (unmodified and modified) has been measured at 77 K and up to 0.1 MPa and presented in Supplementary Fig. 6. A recent study showed that at low temperatures (~20 K) the H_2 forms a super-dense monolayer, up to more than twice that of bulk-solid H_2[38]. With respect to the overall H_2 content of the hydrate phase, the experimental data does not allow for a quantitative assessment. Therefore, the theoretical capacity is estimated in the Supporting Information (See Supplementary Note 1).

The stability tests (Fig. 4, right) confirmed that the clathrates are not degrading even at relatively high temperatures above the heavy water solidification temperature (up to 280 K). Practical applications for safe storage and transport at milder conditions due to the confinement effect and strong interaction with the hybrid material are worth further exploration. This additional exploration is also endorsed by the fact that the N_2-sorption analysis performed after the high-pressure experiments is very similar to the results obtained for the MCFPhene before the clathrate formation (See Supplementary Fig. 7). Note that, during clathrate formation, the ice-like water increases its volume inside the pores of the MCFPhene material. Owing to the thick pore walls of the MCFPhene observed from the electron tomography,

the pore network structure does not collapse, and the material can undergo multiple storage cycles. Besides the relevance of reusability, the fact that more than one cycle can be performed is essential for the induced "memory effect" character when clathrates are formed in nano-confined spaces. Recently, improved kinetics were demonstrated for forming of methane clathrates after the first cycle was performed[20].

According to Nguyen et al., a material must possess four tenable properties to be considered a "nanoreactor" for hydrogen gas hydrates: moderate wettability, medium pore sizes, suitable solid-water interaction, and ice-like molecular arrangement[39,40]. Given the results of our case study, we can assert that all the above-listed requirements are fulfilled. The variation in type and amount of the modifier molecule can accurately adjust the wettability and solid-water interaction. Next, the versatility of the base material MCF allows a vast variation in pore size in the range of mesopores, while its hexagonal symmetry may be regarded as similar to an ice-like structure[37]. Finally, as we recently showed, this material can provide a "memory effect" for gas clathrates formation by substantially accelerating the hydrates' crystallisation after the first cycle. At the same time, the interconnectivity of the pores facilitates the gas hydrates crystallisation[18,20]. With respect to safety and life cycle, clathrate hydrate storage scores very well. While the capacity of adsorbent or hydride storage systems tend to degrade with every use cycle, clathrate hydrates typically benefit from cycling, both in loading kinetics and in water conversion. We have recently demonstrated this for confined CH_4 hydrates[20].

In summary, we have, to the best of our knowledge, proven for the first time that H_2 clathrates can form in hybrid silica materials at lower pressure than what is needed to form bulk H_2O-H_2 hydrate (165 MPa vs 200 MPa). This results from the altered properties of H_2O (D_2O) molecules upon confinement in combination with clathrate-inducing properties of the hydrophobic surface of the hybrid mesoporous silica material. The degree of hydrophobicity induced to the silica walls plays a crucial role by hindering the D_2O to adhere more strongly to the silica walls, thus enhancing hydrate formation. In the conditions presented, nano-confinement reduces the pressure needed for fast H_2 hydrate nucleation by at least 20% as compared to the bulk. More importantly, this type of material offers the advantage of having two sites capable of storing hydrogen, i.e. the clathrate cages and the unmodified silica walls. Stability tests at 280 K and 0.1 MPa showed that confined D_2O-H_2 clathrate hydrate, once formed, remains stable up to 280 K and thus above the solidification temperature of D_2O. Owing to its versatility, silica materials could become a real asset for safe H_2 storage applications, since they are highly stable at the hydrates clathrate formation pressures, and their properties can be tuned explicitly in terms of pore size, interconnectivity between the cavities, surface area and pore volume. The increased stability opens up a new pathway towards multiple-cycles use owing to the "memory effect", which considerably reduces the nucleation time after the first cycle takes place.

Additionally, various molecules to control hydrophobicity can be grafted on the surface. In contrast, accurate densities of molecules per nm^2 can be achieved to make the interface properties easily controllable. However, to reach an "ideal" balance of the surface hydrophobicity for the formation of H_2 hydrates, more extended future experiments are required. Future approaches will explore the grafted molecules containing groups that can act as promoters when used in pure form (THF, cyclopentane, etc.). This material paves the way for a new class of systems capable of storing hydrogen at milder conditions with controlled release over multiple cycles.

Methods

Synthesis of the MCF and surface-modified MCF material

Mesostructured cellular foam (MCF) silica material was obtained following a well-established procedure[41]. The typical methodology involved a template synthesis, with the addition of a swelling agent, namely mesitylene (1, 3, 5-trimethylbenzene). Firstly, the non-ionic triblock copolymer ($EO_{20}PO_{70}EO_{20}$, P123) was dissolved overnight in a solution of H_2O and HCl, at room temperature. Next, the swelling agent together with ammonium fluoride (NH_4F) was added, and the mixture was stirred further for one hour at 308-313 K. Finally, the Si-source, tetraethylorthosilicate (TEOS), was added dropwise, and the white precipitate was stirred for 20 h at 313 K. The hydrothermal treatment involved the transfer of the white precipitate to an autoclave for 24 h, at 373 K. Finally, the mixture was filtrated and washed with distilled water, dried and calcined at 823 K for 6 h, reaching the temperature with a heating rate of 1 K/min. The molar ratio of the precursors was 1 TEOS: 5.87 HCl: 194 H_2O: 0.017 P123: 0.031 NH_4F: 0.815 mesitylene.

Post-synthesis surface modification of the MCF silica material was done with phenethyl trimethoxysilane, following an already reported methodology[42]. Before the procedure, the MCF material was dried overnight at 473 K, then suspended in a toluene solution, while a mixture of toluene and phenethyl trimethoxysilane was added. These steps were performed under an inert atmosphere (Ar flushed) in a glovebox setup, and the mixture was sealed for further stirring for 72 h, at 353 K. Finally, the precipitate was washed several times with toluene to remove the unreacted trimethoxysilane, and dried overnight at 373 K. The resulting material is referred to in the manuscript as MCFPhene.

INS and ND experiments

Inelastic neutron scattering (INS) measurements were performed at the VISION end-station at the Oak Ridge National Laboratory (ORNL). Before the INS measurements, the modified MCF sample (500 mg) was impregnated with D_2O (1.6 g D_2O/g_{silica}). The pre-impregnated sample was loaded into the CuBe cell and pressurised with hydrogen to the desired pressure at 280 K. After a 30 min stabilisation step, the sample cell was cooled down to 5 K to perform the INS analyses. To avoid hydrogen condensation, the cell pressure was released at 160 K. Neutron diffraction measurements were performed in situ using the 90° diffraction detector at VISION. The hydrogen clathrates are formed during the cooling of the hydrogen-loaded samples between 280 K and 160 K, corresponding to a time window of ~2 h according to the recorded cooling curve shown in Supplementary Fig. 1.

Data availability

Source data are provided with this paper. The original data presented in this study are openly available in Harvard Dataverse at: https://doi.org/10.7910/DVN/07U4YK Source data are provided with this paper.

References

1. Schlapbach, L. & Züttel, A. Hydrogen-storage materials for mobile applications. *Nature* **414**, 353–358 (2001).
2. Rahman, A., Farrok, O. & Haque, M. M. Environmental impact of renewable energy source based electrical power plants: Solar, wind, hydroelectric, biomass, geothermal, tidal, ocean, and osmotic. *Renew. Sustain. Energy Rev.* **161**, 112279 (2022).
3. Graetz, J. New approaches to hydrogen storage. *Chem. Soc. Rev.* **38**, 73–82 (2009).
4. Zhou, L. Progress and problems in hydrogen storage methods. *Renew. Sustain. Energy Rev.* **9**, 395–408 (2005).
5. Usman, M. R. Hydrogen storage methods: review and current status. *Renew. Sustain. Energy Rev.* **167**, 112743 (2022).
6. Zhang, L. et al. Fundamentals of hydrogen storage in nanoporous materials. *Progress in Energy* **4**, 42013 (2022).
7. Singh, G. et al. Material-based generation, storage, and utilisation of hydrogen. *Prog. Mater. Sci.* **135**, 101104 (2023).
8. Wang, L. et al. High-pressure hydrogen adsorption in clay minerals: Insights on natural hydrogen exploration. *Fuel* **344**, 127919 (2023).
9. Jaiswal, A., Chakraborty, B. & Sahu, S. A computational insight on the effect of encapsulation and Li functionalization on $Si_{12}C_{12}$

heterofullerene for H_2 adsorption: a strategy for effective hydrogen storage. *ACS Appl Energy Mater.* **6**, 3374–3389 (2023).
10. Rimza, T. et al. Carbon-based sorbents for hydrogen storage: challenges and sustainability at operating conditions for renewable energy. *ChemSusChem* **15**, e202200281 (2022).
11. Mohan, M., Sharma, V. K., Kumar, E. A. & Gayathri, V. Hydrogen storage in carbon materials—a review. *Energy Storage* **1**, e35 (2019).
12. Ramirez-Cuesta, A. J. et al. Dihydrogen in cation-substituted zeolites X - An inelastic neutron scattering study. *J. Mater. Chem.* **17**, 2533–2539 (2007).
13. Ramirez-Cuesta, A. J. et al. Dihydrogen in zeolite CaX-An inelastic neutron scattering study. *J. Alloy. Compd* **446–447**, 393–396 (2007).
14. Zhao, D., Wang, X., Yue, L., He, Y. & Chen, B. Porous metal–organic frameworks for hydrogen storage. *Chem. Commun.* **58**, 11059–11078 (2022).
15. Verma, S. K., Shaz, M. A. & Yadav, T. P. Facile synthesis of M2(m-dobdc) (M = Fe and Mn) metal-organic frameworks for remarkable hydrogen storage. *Energy Storage* **4**, e333 (2022).
16. Suresh, K. et al. Optimizing hydrogen storage in MOFs through engineering of crystal morphology and control of crystal size. *J. Am. Chem. Soc.* **143**, 10727–10734 (2021).
17. Madden, D. G. et al. Densified HKUST-1 monoliths as a route to high volumetric and gravimetric hydrogen storage capacity. *J. Am. Chem. Soc.* **144**, 13729–13739 (2022).
18. Kummamuru, N. B. et al. Accelerated methane storage in clathrate hydrates using mesoporous (Organo-) silica materials. *Fuel* **354**, 129403 (2023).
19. Kummamuru, N. B. et al. Surface modification of mesostructured cellular foam to enhance hydrogen storage in binary THF/H_2 clathrate hydrate. *Sustain Energy Fuels* https://doi.org/10.1039/D4SE00114A (2024) .
20. Beckwée, E. J. et al. Structure I methane hydrate confined in C8-grafted SBA-15: A highly efficient storage system enabling ultra-fast methane loading and unloading. *Appl Energy* **353**, 122120 (2024).
21. Watson, G. et al. Engineering of hollow periodic mesoporous organosilica nanorods for augmented hydrogen clathrate formation. *J. Mater. Chem. A* **11**, 26265–26276 (2023).
22. Gupta, A. et al. Hydrogen clathrates: next generation hydrogen storage materials. *Energy Storage Mater.* **41**, 69–107 (2021).
23. Farrando-Perez, J. et al. Rapid and efficient hydrogen clathrate hydrate formation in confined nanospace. *Nat. Commun.* **13**, 5953 (2022).
24. Beckwée, E. J. et al. Enabling hydrate-based methane storage under mild operating conditions by periodic mesoporous organosilica nanotubes. *Heliyon* **9**, e17662 (2023).
25. Houlleberghs, M. et al. Harnessing nuclear magnetic resonance spectroscopy to decipher structure and dynamics of clathrate hydrates in confinement: a perspective. *Molecules* **29**, 3369 (2024).
26. Breynaert, E. et al. Water as a tuneable solvent: a perspective. *Chem. Soc. Rev.* **49**, 2557–2569 (2020).
27. Liu, Y., Pu, Y. & Zeng, X. C. Nanoporous ices: an emerging class in the water/ice family. *Nanoscale* **15**, 92–100 (2022).
28. Casco, M. E. et al. Experimental evidence of confined methane hydrate in hydrophilic and hydrophobic model carbons. *J. Phys. Chem. C* **123**, 24071–24079 (2019).
29. Casco, M. E. et al. Paving the way for methane hydrate formation on metal-organic frameworks (MOFs). *Chem. Sci.* **7**, 3658–3666 (2016).
30. Casco, M. E. et al. Influence of surface wettability on methane hydrate formation in hydrophilic and hydrophobic mesoporous silicas. *Chem. Eng. J.* **405**, 126955 (2021).
31. Casco, M. E. et al. High-performance of gas hydrates in confined nanospace for reversible CH_4/CO_2 storage. *Chem. – A Eur. J.* **22**, 10028–10035 (2016).
32. Xu, B. & Zhang, Q. Preparation and properties of hydrophobically modified nano-SiO_2 with hexadecyltrimethoxysilane. *ACS Omega* **6**, 9764–9770 (2021).
33. Verma, P., Kuwahara, Y., Mori, K., Raja, R. & Yamashita, H. Functionalized mesoporous SBA-15 silica: recent trends and catalytic applications. *Nanoscale* **12**, 11333–11363 (2020).
34. Morrow, B. A. & McFarlan, A. J. Surface vibrational modes of silanol groups on silica. *J. Phys. Chem.* **96**, 1395–1400 (1992).
35. Wang, X., Du, X., Li, C. & Cao, X. Direct synthesis and characterization of phenyl-functionalized SBA-15. *Appl Surf. Sci.* **254**, 3753–3757 (2008).
36. Thommes, M. et al. Physisorption of gases, with special reference to the evaluation of surface area and pore size distribution (IUPAC Technical Report). *Pure Appl. Chem.* **87**, 1051–1069 (2015).
37. Aktas, O., Yasyerli, S., Dogu, G. & Dogu, T. Structural variations of MCF and SBA-15-like mesoporous materials as a result of differences in synthesis solution pH. *Mater. Chem. Phys.* **131**, 151–159 (2011).
38. Balderas-Xicohténcatl, R. et al. Formation of a super-dense hydrogen monolayer on mesoporous silica. *Nat. Chem.* **14**, 1319–1324 (2022).
39. Nguyen, N. N. & Nguyen, A. V. 'Nanoreactors' for boosting gas hydrate formation toward energy storage applications. *ACS Nano* **16**, 11504–11515 (2022).
40. Nguyen, N. N. Prospect and challenges of hydrate-based hydrogen storage in the low-carbon future. *Energy Fuels* **37**, 9771–9789 (2023).
41. Meynen, V., Cool, P. & Vansant, E. F. Verified syntheses of mesoporous materials. *Microporous Mesoporous Mater.* **125**, 170–223 (2009).
42. Yasmin, T. & Müller, K. Synthesis and characterization of surface modified SBA-15 silica materials and their application in chromatography. *J. Chromatogr. A* **1218**, 6464–6475 (2011).

Acknowledgements

R.-G.C., D A.-E., J.M., S.B. and P.C. acknowledge VLAIO for Moonshot funding (ARCLATH, nr. HBC.2019.0110, ARCLATH2 and nr. HBC.2021.0254). J.S.A. would like to acknowledge financial support from MINECO (PID2019-108453GB-C21), and Conselleria de Innovación, Universidades, Ciencia y Sociedad Digital (Project CIPROM/2021/022). A portion of this research used resources at the Spallation Neutron Source, a DOE Office of Science User Facility operated by the Oak Ridge National Laboratory (project IPTS-29742.1). NMRCoRe acknowledges the Flemish government, department EWI for financial support as International Research Infrastructure (I001321N: Nuclear Magnetic Resonance Spectroscopy Platform for Molecular Water Research).

Author contributions

R-G.C. performed the synthesis and characterisation of the modified silica material. J.F-P. performed the sorption isotherms on the materials. D.A-E. and S.B. performed the electron microscopy experiments and interpretation of the data. L.L.D., J.S.-A. and P.C. performed the INS and ND experiments, and A.J.R.-C., Y.C. and L.L.D. participated in the evaluation and discussion of the INS data. M.H., E.B. and J.M. participated in the evaluation and discussion of the obtained data. R-G.C., P.C. and J.S-A. coordinated the conception and writing of the article. P.C., J. S.-A., S.B. and J.M. were the PIs of the project, and all authors commented on the manuscript and analyses.

Competing interests

The authors declare no competing interests.

Additional information

Supplementary information The online version contains supplementary material available at https://doi.org/10.1038/s41467-024-52893-3.

Correspondence and requests for materials should be addressed to Pegie Cool.

Peer review information *Nature Communications* thanks Erich Müller and the other, anonymous, reviewer(s) for their contribution to the peer review of this work. A peer review file is available.